Coherent Rayleigh-Brillouin Scattering

Xingguo Pan, Mikhail N. Shneider, and Richard B. Miles
Department of Mechanical and Aerospace Engineering, Princeton University, Princeton, New Jersey 08544
(Received 26 April 2002; published 10 October 2002)

Coherent Rayleigh-Brillouin scattering in gases has been studied experimentally for the first time in the kinetic regime and shown to give line shapes that differ significantly from the spontaneous Rayleigh-Brillouin scattering. A kinetic model was developed to obtain an analytic solution of the line shape for monatomic gases, and good agreement with the experimental data was achieved.

DOI: 10.1103/PhysRevLett.89.183001 PACS numbers: 33.20.Fb, 42.50.Vk, 42.65.Hw, 51.10.+y

Spontaneous Rayleigh-Brillouin scattering in gases originates from gas density fluctuations [1]. Its spectrum can be characterized using a uniformity parameter y, which is on the order of the ratio between the scattering wavelength and the gas mean free path. In the kinetic regime, corresponding to y ranging from 0 to around 3, theoretical studies [2–4] usually solve for the gas density fluctuations from kinetic equations. Excellent agreement between experimental data [5–7] and theory has been achieved. It was shown that when $y \to 0$ the scattering light power spectrum is a Gaussian curve corresponding to the Maxwellian distribution function of the gas molecules. As y increases to around one and greater, two shifted peaks appear. Their frequency corresponds to the sound velocity. Recently, efforts have been made to generate perturbations and then probe them with lasers [8–13]. As closely related, coherent Rayleigh scattering studied by Grinstead and Barker [13] is the collisionless limit of the work reported in this Letter. In this Letter, we report the experimental observation of coherent Rayleigh-Brillouin scattering (CRBS) in gases in the kinetic regime. Data obtained in argon and krypton at room temperature and various pressures are presented. We also propose a simple kinetic model that yields good agreement with the experimental data of monatomic gases. We point out that the generated gas density perturbation in our configuration is intrinsically different from the spontaneous fluctuations.

The physical process of CRBS is illustrated in Fig. 1. Two pump beams, $\tilde{\boldsymbol{E}}_1 = \boldsymbol{E}_{10}\cos(\boldsymbol{k}_1 \cdot \boldsymbol{r} - \omega_1 t)$ and $\tilde{\boldsymbol{E}}_2 = \boldsymbol{E}_{20}\cos(\boldsymbol{k}_2 \cdot \boldsymbol{r} - \omega_2 t)$, with the same polarization, are focused and crossed at their foci in the gas. Gas molecules inside the cross region experience dipole forces generated by the inhomogeneity of the intensity field [14]. We choose the x axis along $\boldsymbol{k} = \boldsymbol{k}_1 - \boldsymbol{k}_2$, which is perpendicular to the fringes. The acceleration $a_s(x, t)$ of an individual molecule generated by the two single-mode beams is along the x axis and has a magnitude of

$$a_s = -\frac{\alpha k E_{10} E_{20}}{2M}\sin(kx - \omega t), \qquad (1)$$

where M and α are the mass and polarizability of the gas molecule, respectively; $k = |\boldsymbol{k}|$ and $\omega = \omega_1 - \omega_2$ are the wave number and angular frequency of the dipole force field, respectively. The dipole forces create a wavelike density perturbation in the gas. A third, probe beam is counterpropagated against pump beam 2 and is Bragg scattered off the gas density perturbation. The scattered beam is the CRBS signal. By the phase matching condition, the signal beam follows, in reverse, the path of pump beam 1. The signal maintains the probe beam's polarization and is phase conjugated to pump beam 1. The signal beam's frequency is shifted from the probe beam's by the frequency of the traveling density perturbation wave.

The experimental setup was a modified version of that reported in Ref. [15]. In the experiment, a Q-switched, frequency doubled, broadband, pulsed Nd:YAG laser was used to produce the two pump beams. The power spectrum of the laser has a full width at half maximum of 26.5 GHz with a 250 MHz mode structure modulation. The laser's broadband means that the generated density perturbation is also broadband, i.e., a superposition of waves illustrated in Fig. 1. Therefore, the acceleration $a(x, t)$ of each molecule due to the pump beams is broadband, i.e., a summation of a_s's of all ω. The pump pulse had a duration of about 10 ns and the pulse energy directed into the cross region was around 6 mJ/pulse for each beam. The probe laser was an injection seeded, frequency doubled, pulsed Nd:YAG laser, operated in a single longitudinal mode. Its frequency could be scanned over a range of 20 GHz without mode hopping, and its pulse duration is 7 ns. It was easy to align the optics in the experiment, because the signal is relatively strong. For example, in room air, the signal could be clearly seen by

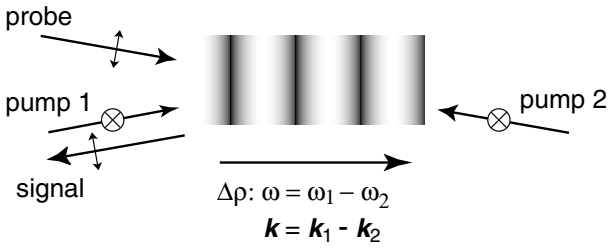

FIG. 1. Coherent Rayleigh-Brillouin scattering in gases.

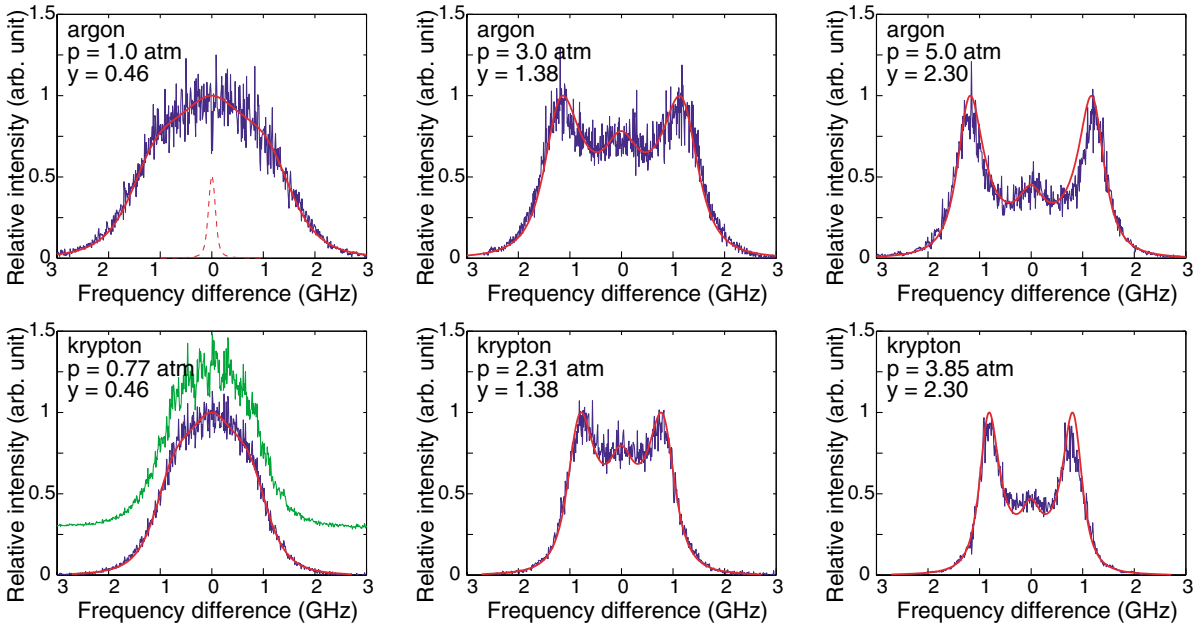

FIG. 2 (color). Power spectrum of coherent Rayleigh-Brillouin scattering at $T_0 = 292$ K in argon and krypton. The blue curve is the experimental data with the pump laser's mode structure filtered out. The red solid curve is a convolution of the theoretical line shape and the instrument function (shown in the argon 1 atm panel by the dashed red curve). The green curve in the krypton 0.77 atm panel is the raw data, offset by 0.3 vertically, displaying the pump laser's mode structure.

eye on a white card with a 1 mJ probe beam pulse energy when the room was dark. The measured signal beam intensity at these conditions was less than 5 μJ. To avoid the complexity of fluctuations generated by the probe and signal beams' interaction, we tuned the probe beam to minimum level in the experiment.

The two pump beams were crossed at their foci inside a gas cell with a 178° angle. The diameter of the focal region was about 200 μm. The paths of the pump beams were carefully arranged so that they arrived at the interaction region simultaneously. The arrival of the probe pulse was adjusted relative to that of the pump pulses so that maximum signal was obtained. The optimal delay was about 1 ns. The jitter of the two lasers was each about 2 ns.

The signal beam was separated from the path of pump beam 1 using a thin film polarizer. It was then propagated for 7 m in the lab to be detected. At this distance, the background ambient scattering of laser light from optical elements was greatly attenuated. About 4% of the signal was directed to a photodetector for normalizing purpose, the rest was detected by another photodetector after passing through an etalon with a free spectra range of 11.85 GHz. The etalon was put in an enclosure whose temperature was stabilized to within ± 0.1 K. In the experiment, the probe laser's frequency was scanned. For each frequency step, the ratio of the signal intensity detected by the photodetector after the etalon to that by the normalizing photodetector made a data point of the line shape. Thirty shots were averaged for each frequency step. The recorded line shape was a convolution of the CRBS line shape and the instrument function. The instrument function was measured by sending the probe laser beam to the detector system and scanning the laser frequency. Shown in the argon 1 atm panel of Fig. 2 is a fitted curve to the average of three measured instrument functions. Also, in each scan, a small portion of the probe laser beam was passed through another 900 MHz etalon to monitor the laser frequency and stability.

Figure 2 shows typical scans in argon and krypton at different pressures, at a temperature of $T_0 = 292$ K. Also indicated is the y parameter for each pressure. The definition of the y parameter is model dependent [3,4]. In this Letter, we use a kinetic model that assumes a constant collision time τ for molecules with different velocities, and the y parameter is defined as

$$y = \frac{1}{k v_0 \tau} = \frac{8}{3\sqrt{2}\pi} \frac{\rho_0 \sqrt{k_b T_0/M}}{\eta k}, \qquad (2)$$

where k_b is the Boltzmann constant, $v_0 = \sqrt{2k_b T_0/M}$, ρ_0 is the average gas density, and $\eta = (1/3)\rho_0 \tau (8k_b T_0/\pi M)$ is the shear viscosity [16]. For the experimental data, y was calculated using the second expression of Eq. (2). The pressure of krypton was chosen to match the y parameter with the argon data. In the context of CRBS line shape, the only significant difference between argon and krypton is their atomic mass. It is expected that the krypton line shape is scalable to the argon line shape for the same y parameter. Our experimental results show that it is indeed the case.

The raw profile for each graph has a 250 MHz modulation due to the pump laser's longitudinal mode

structure. As an example, the raw data in krypton at 0.77 atm is shown by the vertically offset green curve. This modulation was observed as a well-defined, isolated, frequency component in the power spectrum of the recorded profile, and it was filtered out in the frequency domain of the Fourier transform of the recorded data. Data corresponding to smaller y parameters can be found in Refs. [13,15], which showed that the $y \sim 0.02$ curve is about 10% wider than the spontaneous Rayleigh scattering curve. For $y \gtrsim 1$, the coherent Rayleigh-Brillouin spectrum show two strong shifted peaks in addition to the unshifted central peak. The central peak becomes relatively lower as y increases. The shifted peaks correspond to $\omega = kv_s$, where $v_s = \sqrt{\gamma k_b T_0/M}$ is the speed of sound of the gas. The same shape and evolution have also been observed for neon, nitrogen, and carbon dioxide.

We propose a simple kinetic model to explain the observed power spectrum. Since the CRBS is due to the gas density waves driven by the pump beams, its power spectrum is related to the density perturbation by

$$S(k, \omega) \propto \delta\bar{\rho}^*(k, \omega)\delta\bar{\rho}(k, \omega), \tag{3}$$

where k is the wave vector, ω is the angular frequency, and

$$\delta\bar{\rho}(k, \omega) = \frac{1}{2\pi}\iint_{-\infty}^{+\infty} e^{-i(kx-\omega t)}\delta\rho(x, t)dxdt \tag{4}$$

is the space-time Fourier transform of the gas density perturbation.

The gas density perturbation is solved from kinetic equation

$$\frac{\partial f_1}{\partial t} + \boldsymbol{v}\cdot\nabla f_1 + a\frac{\partial}{\partial v_x}(\rho_0 f_0 + f_1) = \frac{1}{\tau}\left[f_0\delta\rho - f_1 + \frac{2\rho_0 f_0}{v_0^2}\boldsymbol{q}\cdot\boldsymbol{v} + \rho_0 f_0\frac{\delta T}{T_0}\left(\frac{v^2}{v_0^2} - \frac{3}{2}\right)\right], \tag{5}$$

where $f_1 = f_1(\boldsymbol{x}, \boldsymbol{v}, t)$ is the deviation from the equilibrium distribution function with $f(\boldsymbol{x}, \boldsymbol{v}, t) = \rho_0 f_0(v) + f_1(\boldsymbol{x}, \boldsymbol{v}, t)$. Other symbols in Eq. (5) are

$$f_0(v) = \frac{1}{\pi^{3/2}v_0^3}\exp\left(-\frac{v^2}{v_0^2}\right), \qquad \delta\rho(\boldsymbol{x}, t) = \int f_1 d^3v, \qquad \boldsymbol{q}(\boldsymbol{x}, t) = \frac{1}{\rho_0}\int \boldsymbol{v} f_1 d^3v,$$
$$\delta T(\boldsymbol{x}, t) = T_0\left[\frac{2}{3\rho_0 v_0^2}\int v^2 f_1 d^3v - \frac{1}{\rho_0}\delta\rho(\boldsymbol{x}, t)\right]. \tag{6}$$

The collision term, i.e., the right-hand side of Eq. (5), is the linearized Bhatnagar-Gross-Krook [17] kinetic model. It has been shown that this model satisfies mass, momentum and energy conservation, and the H theorem. Yip and Nelkin [2] first used this kinetic model to derive an analytic solution of the spontaneous Rayleigh-Brillouin scattering. We take advantage of its simplicity in this study of the CRBS power spectrum. This model considers only the translational movement of the gas molecules; therefore, only monatomic gases will be modeled. The cylindrically symmetric configuration of the experiment allows us to assume along the radial axes a uniform Gaussian distribution that is maintained at the local temperature. The important difference from previous spontaneous scattering consideration is the term $a\frac{\partial}{\partial v_x}(\rho_0 f_0 + f_1)$ in Eq. (5). This term is the forcing term of the gas density perturbation in CRBS and is the key to explain the experimental data. When the perturbation is small, we can simplify Eq. (5) using

$$a\left(\rho_0\frac{\partial f_0}{\partial v_x} + \frac{\partial f_1}{\partial v_x}\right) \approx a\rho_0\frac{\partial f_0}{\partial v_x}. \tag{7}$$

The wavelike steady state solution in the form of $\exp[i(kx - \omega t)]$ can then be found from Eq. (5). Following a procedure similar to that of Ref. [17] and using the traditional dimensionless parameters $\xi = \omega/kv_0$ and y, one obtains the density perturbation as

$$\delta\bar{\rho}(\xi, y) = \frac{i2\rho_0\bar{a}}{kv_0^2}\frac{\mathcal{E}(1 - iy\mathcal{D}) + iy\mathcal{B}\mathcal{F}}{(1 - iy\mathcal{A})(1 - iy\mathcal{D}) + iy\mathcal{B}(1 - iy\mathcal{C})}, \tag{8}$$

where $\bar{a} = \bar{a}(\xi, y)$ is the space-time Fourier transform of the acceleration $a(x, t)$, and

$$\mathcal{A} = (1/\sqrt{\pi})(w_0 + 2\xi w_1),$$
$$\mathcal{B} = (1/2\sqrt{\pi})(-w_0 + 2w_2),$$
$$\mathcal{C} = (2/3\sqrt{\pi})(w_0 + 2\xi w_1 + w_2 + 2\xi w_3),$$
$$\mathcal{D} = (1/3\sqrt{\pi})(w_0 + w_2 + 2w_4), \qquad \mathcal{E} = (1/\sqrt{\pi})w_1,$$
$$\mathcal{F} = (2/3\sqrt{\pi})(w_1 + w_3), \qquad w_4 = (\xi + iy)w_3,$$
$$w_3 = -\sqrt{\pi}/2 + (\xi + iy)w_2, \qquad w_2 = (\xi + iy)w_1,$$
$$w_1 = -\sqrt{\pi} + (\xi + iy)w_0,$$

and

$$w_0(\xi, iy) = \int_{-\infty}^{+\infty}\frac{\exp(-\eta_x^2)}{\xi + iy - \eta_x}d\eta_x$$

is the plasma dispersion function multiplied by $(-\sqrt{\pi})$.

The power spectrum $S(\xi, y)$ can then be calculated from Eqs. (3) and (8). The intensity of coherent Rayleigh-Brillouin scattering signal is proportional to $(\rho_0|\bar{a}|)^2/(kv_0^2)^2$. Its line shape, when the power spectrum of the pump beams is fixed, is independent of the pump beams' intensity in the regime of small perturbation, i.e., when Eq. (7) holds.

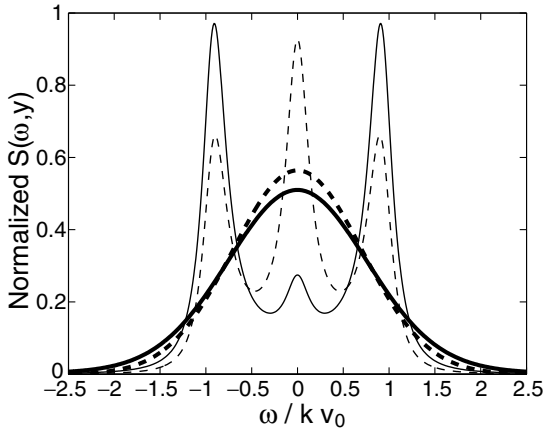

FIG. 3. A comparison between the coherent and spontaneous Rayleigh-Brillouin power spectra calculated from linearized kinetic model, at $y \to 0$ (spontaneous: thick dashed curve, coherent: thick solid curve) and at $y = 3$ (spontaneous: thin dashed curve, coherent: thin solid curve). Area under each curve is normalized to 1.

With a 26.5 GHz pump laser bandwidth in our experiments, $|\bar{a}|$ varies less than 2% over the 6 GHz range of interest and can be considered as a constant, except for the pump laser's mode structure. In Fig. 2, the spectra calculated from Eqs. (3) and (8) for a constant $|\bar{a}|$ are compared with the filtered experimental data. The only adjustment was to match the height at the center of the experimental and theoretical line shapes. Satisfactory agreement was achieved for $y < 1$. At larger y values, the model correctly predicts the position of the Brillouin peaks, but slightly overestimates their height. The scalability of the argon and krypton data and the agreement between theory and experiment show that the physics of CRBS is well described in this regime.

In Fig. 3, we compare the coherent and spontaneous spectra. The difference between the coherent and spontaneous scattering line shapes is because the gas density perturbation in CRBS is generated by a wavelike dipole force field, rather than spontaneous fluctuations. The coherent $y \to 0$ curve is identical to that in Ref. [13], where the curve was obtained by solving a collisionless kinetic equation. The $y = 3$ spontaneous curve was calculated using Yip and Nelkin's [2] formula, which has the same y definition. The important difference at $y \gtrsim 1$ is that the coherent power spectrum has stronger Brillouin peaks and a much weaker Rayleigh peak, indicating that the isentropic sound waves are resonantly pumped by the optical dipole force field. Furthermore, the relative intensity of the Rayleigh peak to the Brillouin doublets becomes smaller as y increases. This is different from the spontaneous case, where the ratio tends to a limit of $(c_p - c_v)/c_v$ [1].

We have shown that the CRBS power spectrum is different from that of the spontaneous scattering. The reason is that the generation of the gas density perturbation has a different mechanism. Our analytical solution of the spectrum based on the kinetic equation agrees well with the experimental data. A more accurate solution of the Boltzmann equation with molecule internal energy considered is desirable for modeling molecular gases as well as for a better agreement with atomic gases experiments. In the kinetic regime, CRBS line shape can be used to measure gas properties and to study gas kinetic processes. It allows us to access gas kinetic processes, previously reached by spontaneous scattering, with a signal that is orders of magnitude stronger. It might also enable us to access new regimes. CRBS has the potential of becoming a new member of Rayleigh scattering based diagnostic methods [18] with the advantages of localized measurement and high signal-to-noise ratio. Interactions between the laser produced dipole force field and the gas molecules provide a possibility of perturbing or transporting ensembles of gas molecules [19].

The authors acknowledge useful discussions with P. F. Barker. This work was supported by the U.S. Air Force Office of Scientific Research under the Air Plasma Rampart program.

[1] L. D. Landau and E. M. Lifshitz, *Electrodynamics of Continuous Media* (Addison-Wesley, Reading, MA, 1966).
[2] S. Yip and M. Nelkin, Phys. Rev. **135**, A1241 (1964).
[3] A. Sugawara, S. Yip, and L. Sirovich, Phys. Fluids **11**, 925 (1968).
[4] G. Tenti, C. D. Boley, and R. C. Desai, Can. J. Phys. **52**, 285 (1974).
[5] T. J. Greytak and G. B. Benedek, Phys. Rev. Lett. **17**, 179 (1966).
[6] N. A. Clark, Phys. Rev. A **12**, 232 (1975).
[7] V. Ghaem-Maghami and A. D. May, Phys. Rev. A **22**, 692 (1980).
[8] C. Y. She *et al.*, Phys. Rev. Lett. **51**, 1648 (1983).
[9] W. A. Schroeder, M. J. Damzen, and M. H. R. Hutchinson, IEEE J. Quantum Electron. **25**, 460 (1989).
[10] S. Williams *et al.*, Opt. Lett. **19**, 1681 (1994).
[11] W. Hubschmid, B. Hemmerling, and A. Stampanoni-Panariello, J. Opt. Soc. Am. B **12**, 1850 (1995).
[12] H. Tanaka, T. Sonehata, and S. Takagi, Phys. Rev. Lett. **79**, 881 (1997).
[13] J. Grinstead and P. F. Barker, Phys. Rev. Lett. **85**, 1222 (2000).
[14] R. W. Boyd, *Nonlinear Optics* (Academic, Boston, 1992).
[15] X. Pan *et al.*, Opt. Lett. **27**, 161 (2002).
[16] L. B. Loeb, *Kinetic Theory of Gases* (Dover, New York, 1961).
[17] P. L. Bhatnagar, E. P. Gross, and M. Krook, Phys. Rev. **94**, 511 (1954).
[18] R. B. Miles, W. N. Lempert, and J. Forkey, Meas. Sci. Technol. **12**, 442 (2001).
[19] P. F. Barker and M. N. Shneider, Phys. Rev. A **64**, 033408 (2001).